MULTISTAGE ALGORITHM FOR LOSSLESS COMPRESSION OF MULTISPECTRAL REMOTE SENSING IMAGES

A. Zamyatin

Tomsk Polytechnic University 30, Lenina ave., Tomsk, 634050, Russia - zamyatin@tpu.ru

KEY WORDS: Multispectral, Compression, Algorithms, Image, Comparison

ABSTRACT:

A preliminary comparison between loss and lossless compression approaches for the remote sensing data processing was made. A three-stage lossless compression algorithm of multispectral remote sensing images based on wavelet transformations and intra-bands correlation is proposed and developed. It allows one to consider peculiarities of remote sensing data and to increase the compression ratio of the algorithm. The paper describes a modification of the compression algorithm aimed at considerable improvement of computational performance and based on bands trimmed enumeration and data selective use. A research of the three-stage algorithm performance was carried out in comparison with the universal compression algorithms such as *WinRar*, *WinZip* and *JPEG2000* using data from various remote sensing systems showing to some extent a superiority in the compression ratio, as well as some insignificant lag of the computational performance was identified.

1. INTRODUCTION

Due to the constantly improving technical features of remote sensing (RS) systems and the extended use of RS data for solving various tasks, the data amount handled by RS modern systems is in terabytes and it continues to increase steadily. Hence, the resolution of RS data compression problems using different approaches, software and hardware aimed at increasing the effectiveness of data processing, storage and transmission along communication channels is becoming more relevant (Cagnazzo etc., 2006; Marcellin etc., 1995; Motta etc., 2006; Salmon, 2007; Ziv & Lempel, 1977). In general, data compression approaches can be presented by loss and lossless ways. Let us consider first a possibility to use the lossless approach for RS data compression.

Lossy algorithms are widely used for image compression tasks and are characterized by high possible compression ratio (Jacquin, 1993). For instance, the most popular algorithms are based on fractal approach and are used both for color and grayscale images without a sharp color change (for example, photo pictures). It allows one getting high compression rates over 200. The fractal algorithm might be implemented for each RS band of $N \times M$ size and it is based on the so called *domain* and *rang* regions (areas) processing (Fig. 1).
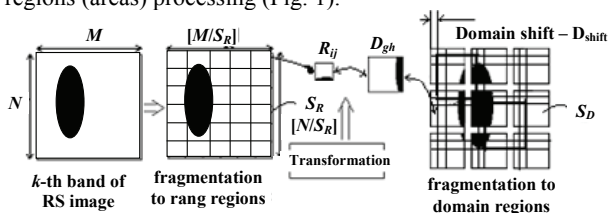

Figure 1. A general scheme of the fractal algorithm

The fractal algorithm could bring a significant compression ratio for the large images that are common for RS images. The rang regions are non-overlapping image fragments, the sum of which fully covers the image. Domain regions are similar to the rang regions. They are also formed by an image decomposition to some equivalent grid but differ in a bigger size and a shift. Detailed description of fractal algorithm for image compression

can be found in (i.e. Jacquin, 1993), but briefly it could be generally presented in the following way:

1. Decompose the image by equivalent grid to the same set of square rang regions R_{ij} with S_R number of elements (pixels) where $i = 0, S_R,..., ([M/S_R] - 1) \times S_R; j = 0, S_R,..., ([N/S_R]-1) \times S_R$.

2. Form D_{gh} domain regions with S_D dimension, where $g = 0, D_{shift}, 2 \times D_{shift}, ..., [(M - S_D)/D_{shift}] \times D_{shift}; h = 0, D_{shift}, 2 \times D_{shift}, ..., [(N - S_D)/ D_{shift}] \times D_{shift}$.

3. For every R_{ij} element search through all D_{gh} elements and form $R_{ij} \rightarrow D_{gh}$ affine transformation:

$$f_k(x, y, I(x,y)) = \begin{pmatrix} a & b & 0 \\ c & d & 0 \\ 0 & 0 & p \end{pmatrix} \times \begin{pmatrix} x \\ y \\ I(x,y) \end{pmatrix} + \begin{pmatrix} u \\ v \\ q \end{pmatrix},$$

where $k = 1, 2, ..., k_{af}$ – the number of affine transformation, x,y – coordinates of image pixel, $I(x,y)$ – pixel brightness with (x,y) coordinates, p – a coefficient that is called brightness (operating with grayscale image $p = 1$), a, b, c, d – coefficients oriented on performing the rotation and reflecting symmetry, u,v – shift of the point with (x,y) coordinates along the axes, q – coefficient that is called the shift of brightness point with (x,y) coordinates and is calculated as:

$$q = [\sum_{m=1}^{S_R} \sum_{l=1}^{S_R} r_{ml} - \sum_{m=1}^{S_R} \sum_{l=1}^{S_R} d_{ml}]/n^2,$$

where m, l – pixel coordinates, $r_{ml} - I(m, l)$ in R_{ij} rang region, $d_{ml} - I(m, l)$ in D_{gh} domain region.

4. Choose from all transformations one with the least error, calculated as:

$$d = \sum_{m=1}^{S_R} \sum_{l=1}^{S_R} [(r_{ml} - d_{ml}) - q]^2.$$

5. Fix the number of k_{af}, coordinates of the top-left corner of R_{ij} rang region, q shift of brightness in file.

The described fractal algorithm consequently implements the compression for every band of a multispectral RS image.

To evaluate the application outlook of the proposed lossy compression algorithm it is implemented in a framework of the fractal approach, some test experiments were performed. They revealed that the loss compression algorithm could provide

In: Wagner W., Székely, B. (eds.): ISPRS TC VII Symposium – 100 Years ISPRS, Vienna, Austria, July 5–7, 2010, IAPRS, Vol. XXXVIII, Part 7A

| Contents | Author Index | Keyword Index |

rather high compression ratios. A visual evaluation comparison between the initial and the uncompressed RS images (example on Fig. 2a,b) demonstrated a possibility to use the uncompressed RS images for the manual visual interpretation in some cases.
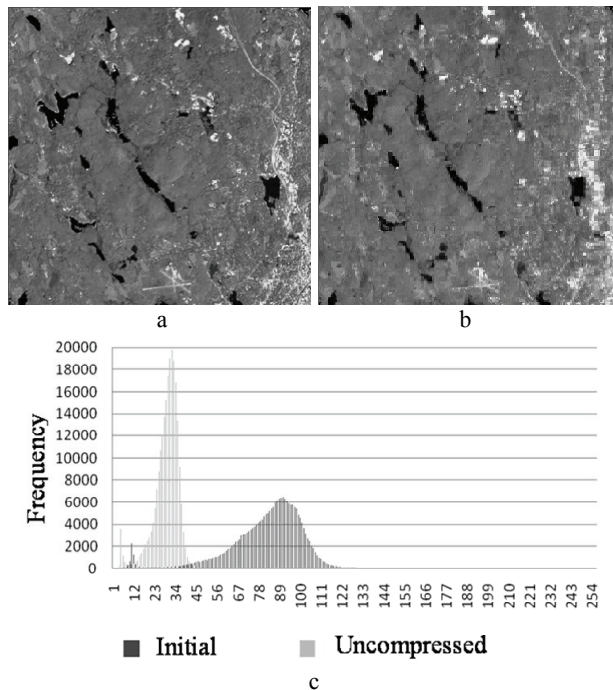

Figure 2. Results of lossy compression: original multispectral RS (a), uncompressed RS image (b), histograms of a RS band (c)

At the same time a comparison of the frequency brightness histograms proves the significant changes in statistic brightness characteristics of the uncompressed RS image in comparison with the initial RS one (Fig. 2c). That implies possible difficulties in further automatic processing and classification of these uncompressed RS data, though high compression rates could be provided.

Thus, taking into account a possible demand in RS data preliminary processing and automated classification it is more reasonable to avoid distortion of statistical albedo characteristics of uncompressed RS images. It is possible to avoid with lossless compression algorithms which are considered most valuable for the RS data processing.

There are two conceptually different approaches to the RS data lossless compression. One approach implies the use of the universal and well-known compression algorithms do not take into account the specific features of RS data and which is represented in such software as *WinRar*, *WinZip* or which uses the compression standard of black-and-white and colored images as *JPEG2000* (Christopoulos, 2001; Taubman & Marcellin, 2002; Salmon, 2007;). Another approach is focused on new compression algorithms which take into account not only bands data as simple black-and-white images, but also relation between RS image bands. In spite of the fact that such approach is more complex from computational point of view its application allows one to achieve considerable compression ratio due to specific features of RS data.

In this respect the paper is aimed at the development and research of multispectral algorithms of lossless RS images compression based on both independent data processing in different bands and considering their intra-bands correlation to improve the compression ratio in comparison with well-known universal compression algorithms.

2. THREE-STAGE COMPRESSION ALGORITHM

The wavelet transformations allow one to obtain coefficients which can be compressed significantly better than initial image data. This approach to the lossless image compression is considered as the most efficient one (Salmon, 2007; Christopoulos, 2001). Multispectral RS images represent albedo values obtained in different spectral bands and which as a rule have considerable intra-bands correlation. If such functional relation is known it is possible to considerably decrease data transformation range using deviation (difference) values between the functional relation and the actual initial values. This will allow one to use significantly less number of bits to store such deviations than it is necessary to store the initial RS data. Eventually this allows one to increase the final compression ratio.

The application of the abovementioned transformations in the compression allows one to use the advantages of the wavelet transformations and the existing relation between the bands of multispectral RS images. Taking this into account, the compression algorithm can be carried out in three stages:

- to carry out wavelet transformation of initial data and obtaining corresponding transformation coefficients;
- to consider functional relation of albedo values between different image bands and to form a set of data deviations;
- to compress obtained data using one of the traditional compression algorithms.

Let us consider the stages of the suggested three-stage compression algorithm of multispectral RS images in detail.

The wavelet transformation is applied to an initial RS image according to rows and columns with given number of levels thus setting high-frequency and low-frequency components (Fig. 3).
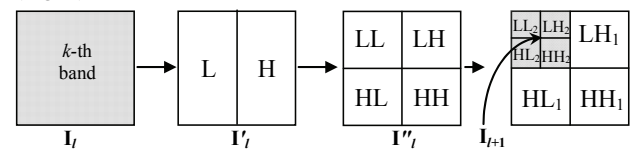

Figure 3. High-frequency and low-frequency components in wavelet transformation from RS image k-band data

To describe the first stage of compression algorithm step-by-step it is necessary to identify the following notational conventions: M – number of rows, N – number of columns, K – number of initial multispectral RS bands, l – an index of the current transforming level, L – number of transforming levels, sign "$\lfloor \ \rfloor$" – rounding up to the integer number.

Step 1. Set $m = 0$, $n = 0$, $k = 1$, $l = 1$.

Step 2. Obtain even $\mathbf{I}_l[m, 2j, k]$ and uneven $\mathbf{I}_l[m, 2j+1, k]$ components at $j = 0, 1, …, \lfloor N/2^l \rfloor$ from the initial image $\mathbf{I}_l[m, n, k]$.

Step 3. Calculate low-frequency $\mathbf{Y}[m, 2j]$ and high-frequency $\mathbf{Y}[m, 2j+1]$ components by using 5 and 3 summand components of the initial image $\mathbf{I}_l$, at $j = 0, 1, …, \lfloor N/2^{l-1} \rfloor$:

$\mathbf{Y}[m, 2j] = (- \mathbf{I}_l[m, 2j-1, k] + 2 \cdot \mathbf{I}_l[m, 2j, k] + 6 \cdot \mathbf{I}_l[m, 2j+1, k] + 2 \cdot \mathbf{I}_l[m, 2j+2, k] - \mathbf{I}_l[m, 2j+3, k])/8,$

$\mathbf{Y}[m, 2j+1] = (- \mathbf{I}_l[m, 2j, k] + 2 \cdot \mathbf{I}_l[m, 2j+1, k] - \mathbf{I}_l[m, 2j + 2, k])/2$ or after approximation and rounding up operations

$\mathbf{Y}[m, 2j] = \mathbf{I}_l[m, 2j, k] + \lfloor (\mathbf{Y}[m, 2j-1] + \mathbf{Y}[m, 2j + 1]) + 2)/4 \rfloor,$

$\mathbf{Y}[m, 2j + 1] = \mathbf{I}_l[m, 2j + 1, k] - \lfloor (\mathbf{I}_l[m, 2j, k] + \mathbf{I}_l[m, 2j+2, k])/2 \rfloor$

Step 4. If $m < M$ then $m = m + 1$, step 2, otherwise step 5.

Step 5. Form the image $\mathbf{I}'_l$, containing high-frequency and low-frequency areas (according to columns):

In: Wagner W., Székely, B. (eds.): ISPRS TC VII Symposium – 100 Years ISPRS, Vienna, Austria, July 5–7, 2010, IAPRS, Vol. XXXVIII, Part 7A

Contents   Author Index   Keyword Index

For $p = 0, 1,…, \lfloor M/2^{l-1}\rfloor$, $q = 0, 1,…, \lfloor N/2^l\rfloor$, $\mathbf{I}'_l[p, q, k] = \mathbf{Y}[m, 2j]$;

For $p = 0, 1,…, \lfloor M/2^{l-1}\rfloor$, $q = \lfloor N/2^l\rfloor + 1, \lfloor N/2^l\rfloor + 2,…,\lfloor N/2^{l-1}\rfloor$, $\mathbf{I}'_l[p, q, k] = \mathbf{Y}[m, 2j+1]$.

Step 6. Calculate low-frequency $\mathbf{Y}[m, 2j]$ and high-frequency $\mathbf{Y}[m, 2j + 1]$ components on the basis of $\mathbf{I}'_l$:

$\mathbf{Y}[2j, n] = \mathbf{I}'_l[2j, n, k] + \lfloor(\mathbf{Y}[2j-1, m] + \mathbf{Y}[2j + 1, n]) + 2)/4\rfloor$,

$\mathbf{Y}[2j + 1, n] = \mathbf{I}'_l[2j+1, n, k] - \lfloor(\mathbf{I}'_l[m, 2j, k] + \mathbf{I}'_l[m, 2j + 2, k])/2\rfloor$.

Step 7. If $n < N$ then $n = n + 1$, step 6, otherwise step 8.

Step 8. Form the image containing high-frequency and low-frequency areas (according to rows):

$\mathbf{I}''_l[p, q, k] = \mathbf{Y}[2j, q]$ at $p = 0, 1,…, \lfloor M/2^{l-1}\rfloor$ for $q = 0, 1,…, \lfloor N/2^{l-1}\rfloor$;

$\mathbf{I}''_l[p, q, k] = \mathbf{Y}[2j+1, q]$ at $p = \lfloor M/2^{l-1}\rfloor + 1, \lfloor M/2^{l-1}\rfloor + 2, …, \lfloor M/2^l\rfloor$ for $q = 0, 1,…, \lfloor N/2^{l-1}\rfloor$.

Step 9. For $p = 0, 1,…, \lfloor M/2^{l-1}\rfloor$ and $q = 0, 1,…, \lfloor N/2^{l-1}\rfloor$ form $\mathbf{I}^w_l[p, q, k] = \mathbf{I}''_l[p, q, k]$, if $l < L$ then $l = l + 1$, step 2, otherwise step 10.

Step 10. If $k < K$ then $k = k + 1$, step 2, otherwise step 11.

Step 11. End.

The result of this stage is the image $\mathbf{I}^w_l[m, n, k]$ containing obtained low-frequency and high-frequency components found on the basis of the initial image $\mathbf{I}[m, n, k]$ using wavelet transformation with L levels of depth.

The main point of the second stage is to consider band-to-band correlation by defining the deviations between an obtained functional relation (of the 1st order in the given case) and the actual values in corresponding bands data obtained at the first stage by the wavelet transformation. Storage and further processing of deviations (not the initial data) is characterized by considerably low value change range, which requires the less number of bits and will allow one to compress such data with the higher ratio. The diagram of such transformation is shown in Fig. 4.

Given that $\mathbf{I}^Q_l[m, n, k]$ – matrix of $\mathbf{I}^w_l[m, n, k]$ image quadrant values with index Q, $Q = \{LL, LH, HL, HH\}$, $e_l[m, n, k]$ – deviation matrix, then step-by-step description of the compression algorithm second stage can be presented in the following way:

Step 1. For $m = 0,1,…,M$, $n = 0,1,…,N$, $Q = \{LL,…, HH\}$,

$e^Q_L[m, n, 1] = \mathbf{I}^Q_L[m, n, 1]$,

$e^{LL}_L[m, n, 2] = \mathbf{I}^{LL}_L[m, n, 2] - \mathbf{I}^{LL}_L[m, n, 1]$.

Step 2. For $m = 0, 1,…, \lfloor M/2^l\rfloor$, $n = 0, 1,…, \lfloor N/2^l\rfloor$, $k = 3,4,…,K$, $e^{LL}_L[m,n,k] = \mathbf{I}^{LL}_L[m,n,k] - 2\cdot\mathbf{I}^{LL}_L[m, n, k-1] + \mathbf{I}^{LL}_L[m, n, k-2]$.

Step 3. Calculate coefficients for L level:

$\mathbf{w}^{LH}_L[k] = (\mathbf{J}^{LL}_L[k]^T \times \mathbf{J}^{LL}_L[k])^{-1} \times \mathbf{J}^{LL}_L[k]^T \times \mathbf{J}'^{LL}_L[k]$, $\mathbf{J}_L$ – m by n matrix $Z \times (\lfloor M/2^{L-1}\rfloor+1) \times (\lfloor N/2^{L-1}\rfloor+1)$, where $Z = 2$ at $k<2$, otherwise $Z = 1$.

$\mathbf{J}^{LL}_L[k] = [[\mathbf{I}^{LL}_L[0, 0, k-1], [\mathbf{I}^{LL}_L[0, 1, k-1], …, \mathbf{I}^{LL}_L[\lfloor M/2^{L-1}\rfloor, \lfloor N/2^{L-1}\rfloor, k-1], [\mathbf{I}^{LL}_L[0, 0, k-2], [\mathbf{I}^{LL}_L[0, 1, k-2], …, \mathbf{I}^{LL}_L[\lfloor M/2^{L-1}\rfloor, \lfloor N/2^{L-1}\rfloor, k-2]]$, $\mathbf{J}'^{LL}_L[k]$ – vector with length $(\lfloor M/2^L\rfloor+1)\times(\lfloor N/2^L\rfloor+1)$, $\mathbf{J}'^{LL}_L[k] = [[\mathbf{I}^{LL}_L[0, 0, k], [\mathbf{I}^{LL}_L[0, 1, k], …, \mathbf{I}^{LL}_L[\lfloor M/2^{L-1}\rfloor, \lfloor N/2^{L-1}\rfloor, k]]$, where "T" – matrix transforming character, "–1" – inverse matrix character.

Step 4. For $l = L, L-1, L-2,…,1$ calculate other vectors of coefficients $\mathbf{w}^{LH}_l$ and coefficients $\mathbf{w}^{HL}_l$, $\mathbf{w}^{HH}_l$:

$\mathbf{w}^{LH}_l[k] = [(\mathbf{J}^{HH}_{l-1}[k]^T \times \mathbf{J}^{HH}_{l-1}[k])^{-1} \times \mathbf{J}^{HH}_{l-1}[k]^T \times \mathbf{J}'^{HH}_{l-1}[k])]$,

$\mathbf{w}^{HL}_l[k] = [(\mathbf{J}^{LH}_l[k]^T \times \mathbf{J}^{LH}_l[k])^{-1} \times \mathbf{J}^{LH}_l[k]^T \times \mathbf{J}'^{LH}_l[k])]$,

$\mathbf{w}^{HH}_l[k] = [(\mathbf{J}^{HL}_l[k]^T \times \mathbf{J}^{HL}_l[k])^{-1} \times \mathbf{J}^{HL}_l[k]^T \times \mathbf{J}'^{HL}_l[k])]$.

Step 5. For $l = 1,2,…,L$ and $Q = \{LH, HL, HH\}$ find

$$\boldsymbol{e}^Q_l[m,n,k] = \mathbf{I}^Q_l[m,n,k] - (\mathbf{w}^Q_l[k])^T \times \begin{pmatrix} \mathbf{I}^Q_l[m,n,k-1] \\ \mathbf{I}^Q_l[m,n,k-2] \end{pmatrix}.$$

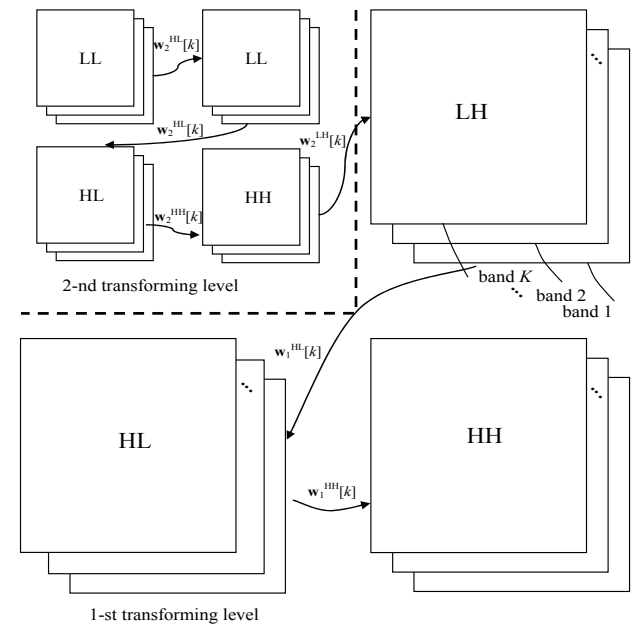*Step* 6. If $k < K$ then $k = k + 1$, step 4, otherwise step 7.

Step 7. End.

Figure 4. Generalized scheme of intra-bands correlation for transforming levels $l = 1$ and $l = 2$

The result of the second stage is deviation matrix $e_l[m,n,k]$, which can be compressed by some algorithm at the final stage. In this case it is suggested to use a well-known arithmetical algorithm to compress the obtained data (Salmon, 2007; Witten etc., 1987).

To form the uncompressed multispectral image $\mathbf{I}[m,n,k]$ out of $e_l[m,n,k]$ it is necessary to carry out a number of transformations opposite the above mentioned ones.

3. EXPERIMENTS

To define the efficiency of the suggested three-stage algorithm from the point of view of compression ratio and computational performance, as well as its validity limits, numerous experiments using multispectral RS images of different RS data systems (Table 5) in data format of raster geoinformation system *Idrisi Kilimanjaro* were carried out together with their comparison with experimental results obtained for well-known prototypes – *WinRar*, *WinZip* and *JPEG2000* of *FastStone Image Viewer* (Salamon, 2007; Kiely etc., 2006; Christopoulos etc., 2001). The algorithm was implemented in *Borland Developer Studio 2006* without special attention to the code optimization. That is why there are spaces for possible improvements. Experiments were carried out on *Intel Pentium IV* PC, 2.8 GHz, 1 Gb memory under *Windows XP* (SP 3).

In: Wagner W., Székely, B. (eds.): ISPRS TC VII Symposium – 100 Years ISPRS, Vienna, Austria, July 5–7, 2010, IAPRS, Vol. XXXVIII, Part 7A

Contents   Author Index   Keyword Index

No.	RS data systems	Number of bands	Size of image, pixels	Size of file, bytes
1	SPOT	3	509 × 571	871917
2	SPOT	3	615 × 558	1029510
3	ADAR–5000	3	541 × 440	714120
4	Airphoto	3	652 × 694	1357464
5	Landsat–MSS	4	558 × 560	1249920
6	Landsat–MSS	4	480 × 480	921600
7	Landsat–TM	6	934 × 700	3922800
8	Landsat–TM	7	500 × 500	1750000
9	Landsat–TM	7	525 × 280	1029000
10	Flightline C1	12	949 × 220	2505360

Table 5. RS experimental data

As was mentioned above, one of the key parameters of the wavelet transformation is its L depth which can be set over in a wide range. The increase of L value might lead to an increase of the compression ratio due to making greater high-frequency area. To define the most acceptable range of L parameter a number of experiments were carried out, the results of which are shown in Fig. 3.
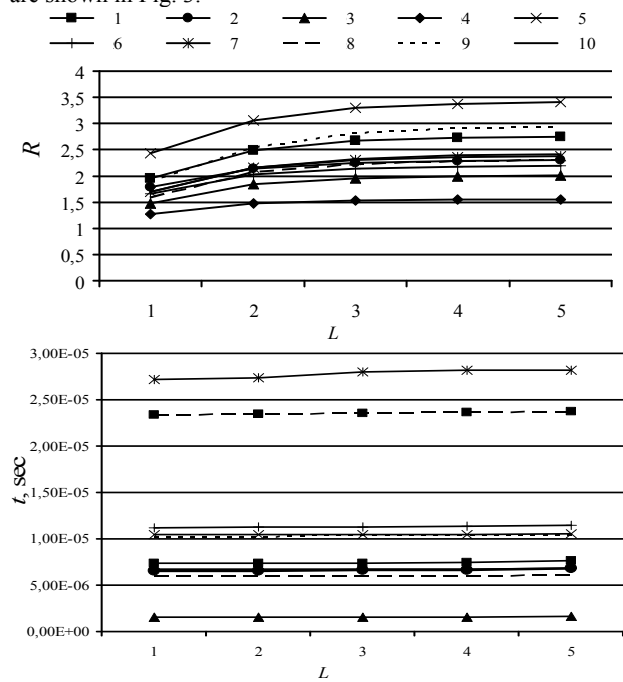

Figure 6. Relation of compression ratio and time on wavelet transformation with depth L

Experimental results presented in Fig. 6 show that although algorithm computational performance for $L \in [1;5]$ does not depend much on the transformation depth the compression ratio R ceases to increase even at $L \geq 3$. Due to this it is advisable to accept here $L = 3$.

It is obvious that at the result of the second stage of the algorithm are the deviations e_l obtained with functional relation (set by coefficients $\mathbf{w}_l^{LH}$, $\mathbf{w}_l^{HL}$, $\mathbf{w}_l^{HH}$) from the values of a transformed image band. Hence, data compression ratio may depend on the order of bands processing. Some experimental results

confirming this point are shown in Fig. 7. As we can see, the compression ratio at the most "successful" (the "best") order of bands processing is considerably (by 10-15%) higher than the compression ratio obtained for the same data at the "worst" order of bands processing.

One of the methods to define the most "successful" (suitable) combination of bands processing can be the enumeration of all possible combinations characterized by the need to carry out $K!$ compression operations with initial image and hence, by considerable computational expenses. To reduce computational expenses while defining the most "successful" order of bands processing it is suggested to use a method of "trimmed" bands enumeration. The method includes sequential increase in the number of bands wherein combination of 2 elements taken K at a time, then combination of 3 elements taken K at a time, etc. is subject to maximum compression ratio.
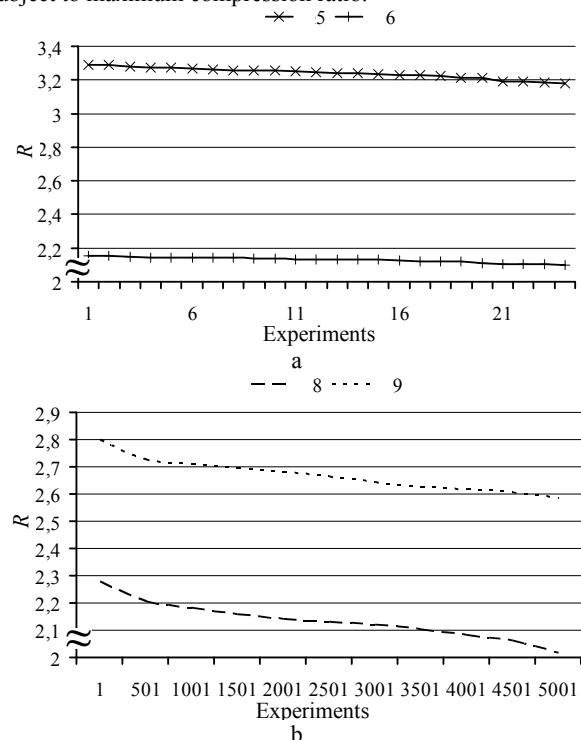

Figure 7. Compression ratio of multispectral RS images vs. different orders of bands enumeration and processing: $K \geq 3$ (*a*), $K \geq 7$ (*b*).

The algorithm of such trimmed enumeration given that vector with the length K, each element of which presents the number of a corresponding band processing in a corresponding position and can be shown in the following way:

Step 1. Set initial length of sub vectors v_i as $S=2$, $i=1,2,…,C_S^K$, where C_S^K – the number of combinations of K elements taken S at a time.

Step 2. If $S = 2$ is formed from the initial vector $\mathbf{V}$ all possible sub vectors v_i with numbers of S length bands processing order.

Step 3. If $S > 2$ is formed from sub vector v_i^{max} and every remaining bands of $\mathbf{V}$ vector all possible S length sub vectors v_i.

Step 4. For all i carry out compression using three-stage algorithm taking into account bands processing order set in sub vectors v_i.

Step 5. Out of all v_i find sub vector v_i^{max} with maximum compression ratio.

Step 6. If $S < K–1$, then $S=S+1$, step 3, otherwise step 7.

Step 7. End.

In: Wagner W., Székely, B. (eds.): ISPRS TC VII Symposium – 100 Years ISPRS, Vienna, Austria, July 5–7, 2010, IAPRS, Vol. XXXVIII, Part 7A

Contents   Author Index   Keyword Index

K length sub vector v_i containing obtained (the "best") order of bands processing will be the result of the algorithm.

It is evident that the "best" order of bands processing obtained by this method can be different from the one obtained via complete enumeration of possibilities but at the same time it requires the less number of operations. In order to prove this point of view and to assess the compression ratio R of different test RS images a number of experiments was carried out, the results of which are shown in Fig. 6.

It is noteworthy that the RS image no.10 was excluded from the experiments due to practical impossibility to process 12 bands simultaneously. Obtained results demonstrate the advantage of trimmed enumeration in defining the processing order before any other method from the point of view of computational performance and compression ratio (in some cases slightly yielding to the maximum possible compression ratio obtained when using the completed enumeration of processing possibilities).
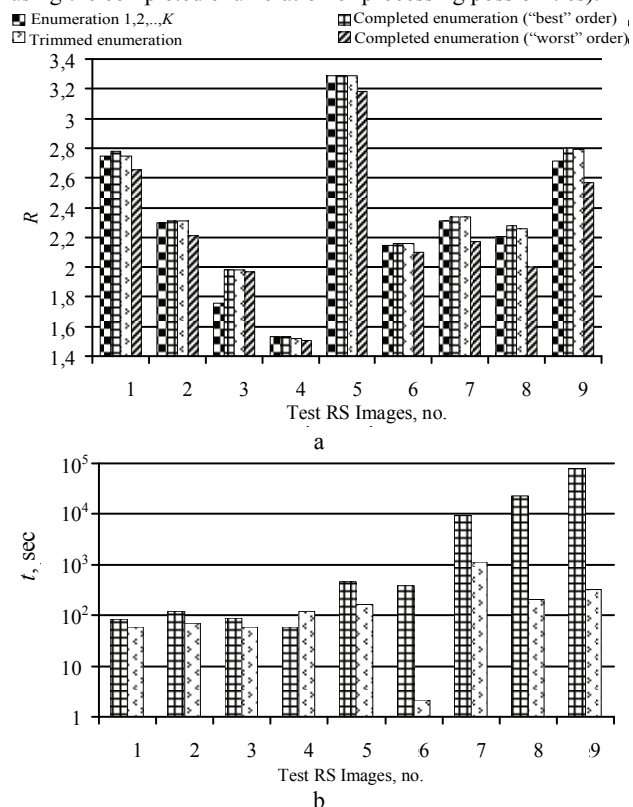

Figure 8. Relation of compression ratio and time on the way of bands processing order when identifying the "best" combination

Besides, when the number of image bands $K>4$ the advantage of the suggested method of trimmed enumeration becomes multiple, particularly for RS images of larger geometrical size (image no.6, Fig.*b*). The results presented in Fig. *b* show that even the use of trimmed enumeration might require dozens of seconds during compression, which cannot be considered satisfactory for practical purposes.

In order to increase the computational performance of defining the "best" order of bands processing it is suggested to modify the above considered trimmed enumeration algorithm by the selective data processing where step 4 should be applied not for the whole initial image but it is advisable to use randomly selected data samples of a specified size.
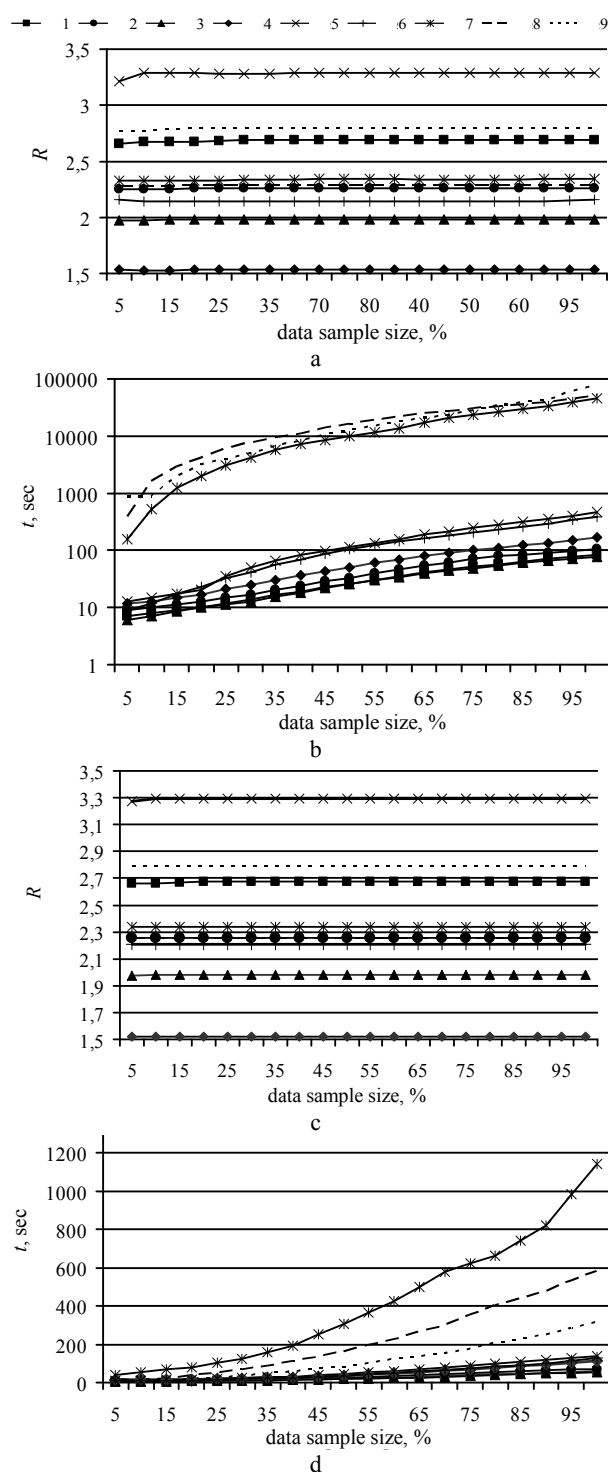

Figure 9. Relation of compression ratio and computational performance vs. data set size at completed (*a,b*) and trimmed (*c,d*) enumeration of bands

The results justify greater computational performance of the trimmed enumeration with the selective data use in compari Comparative investigation results of the prototypes and the modified algorithm based on methods of the trimmed enumeration, processing of bands and selective data processing with different data sample size are shown in Fig. 9.

son with the completed enumeration, as well as research allows one to make a conclusion on the fact that in order to define the "best" bands order processing it is enough to use lossless compression with a data sample size containing 8-10% of pixels of

In: Wagner W., Székely, B. (eds.): ISPRS TC VII Symposium – 100 Years ISPRS, Vienna, Austria, July 5–7, 2010, IAPRS, Vol. XXXVIII, Part 7A

| Contents | Author Index | Keyword Index |

initial data. In this case multiple increase of the computational efficiency (7÷40 times) is achieved. Thus, higher computational performance are typical for the images with more bands and greater geometrical size of scene. Based on experimental results and conclusions let us accept the use of selection equal 10% sufficient for the suggested modified algorithm.

The peculiar feature of the suggested compression algorithm is a joint use of wavelet transformations taking into account intra-bands correlation and some original modifications on search of the suitable order of the bands processing. The algorithm might increase possible compression ratio and improve computational performance. This allows one to advance universal *WinRar*, *WinZip* or *JPEG2000*, which do not consider peculiarities of multispectral RS images. However, the results of carried out comparative experiments presented in Fig. 10 show that suggested modifications of the compression algorithm and the selective data use with a various sample data size allow one to make the computational performance of the three-stage algorithm slightly comparable with *WinRar*, *WinZip* and *JPEG2000*, but at the same time more competitive in terms of compression ratio.
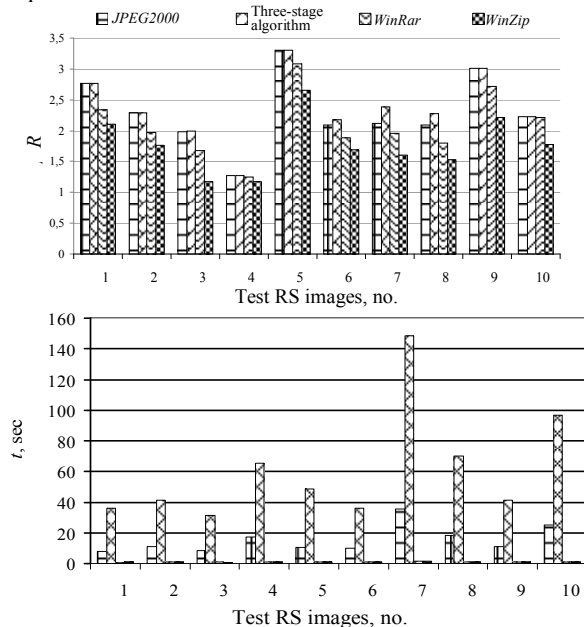

Figure 10. Comparative efficiency of the different compression algorithms

4. CONCLUSIONS

The three-stage compression algorithm of multispectral RS images based on the use of wavelet transformations and intra-bands correlation was developed. Data test set included 10 multispectral RS images of different RS systems was used for its research on a computational performance, compression ratio and validity. It allows one to define the ideal depth of wavelet transformation $L=3$, as well as to identify the relation of a compression ratio and time with the different ways of bands processing order while looking for the "best" bands combination from a view point of a maximum possible compression ratio. In order to increase the computational performance the algorithm was modified by a trimmed enumeration of the bands processing and data selective use, as well as the sufficient sample size equal 10% is identified. The overall computational performance increased in 7÷40 times, and compression ratio – on 15-20% in comparison with non-modified prototype.

The comparative research of the three-stage compression algorithm with universal *WinRar*, *WinZip* and *JPEG2000* was carried out taking into account all modifications and found parameters of the algorithm. Results allow one to make the conclusion on the considerable advantage of the suggested modified algorithm if compared it with its prototypes in terms of compression ratio but with some disadvantage in computational performance.

REFERENCE

Cagnazzo, M., Cicala, L., Poggi, G., Verdoliva, L., 2006. Low-complexity compression of multispectral images based on classified transform coding. *Signal Processing: Image Communication*. 10 (21), pp. 850-861.

Christopoulos, C., Skodras, A., Ebrahimi, T., 2001. The JPEG2000 still image coding system. *Signal Processing Magazine, IEEE*. 5(18), pp. 36-58.

Jacquin, A., 1993. Fractal Image Coding: A review. In: *Proceedings of the IEEE*, Vol. 81, pp 1451-1465.

Kiely, A., Klimesh, M., Xie, H., Aranki, N., 2006. ICER-3D: A Progressive Wavelet-Based Compressor for Hyperspectral Images. The Interplanetary Network Progress Report, pp. 142-164.

Marcellin, M., Abousleman, G., Hunt, B., 1995. Compression of hyperspectral imagery using the 3d dct and hybrid dpcm/dct. *J IEEE Transactions on Geoscience and Remote Sensing*, 33(1), pp. 26-35.

Motta, G., Rizzo, F., Storer J.A., 2006. *Hyperspectral Data Compression*. Springer, US, XI, 415 p.

Salmon, D., 2007. *Data Compression*. Springer-Verlag Ltd., London, p.1074

Taubman D., Marcellin M., 2002. *JPEG2000: Image Compression Fundamentals, Standard and Practice.* Kluwer Academic Publishers, Massachusetts, 808 p.

Witten, I., Neal, R., Cleary, J., 1987. Arithmetic coding for data compression. *J Communications of the ACM*. 30, pp. 520-540.

Ziv, J., Lempel, A., 1977. A universal algorithm for sequential data compression. *IEEE Transactions on Information Theory*. 23, pp. 337-343.